



The fractionation of adipose tissue procedure to obtain stromal vascular fractions for regenerative purposes

Joris A. van Dongen, BSc^{1,2,3}; Hieronymus P. Stevens, MD, PhD¹; Mojtaba Parvizi, DVM, PhD²; Berend van der Lei, MD, PhD^{3,4}; Martin C. Harmsen, PhD²

1. Plastic Surgery Department, Bergman Clinics, Rijswijk, The Netherlands,
2. Department of Pathology & Medical Biology,
3. Department of Plastic Surgery, University of Groningen and University Medical Centre of Groningen, Groningen, The Netherlands, and
4. Plastic Surgery Department, Bergman Clinics, Heerenveen and Zwolle, The Netherlands

Reprint requests:

Dr. Hieronymus P. Stevens, MD, PhD,
Bergman Clinics, Rijswijk Braillelaan 5
2289 CL, Rijswijk, the Netherlands.
Tel: +31624810440;
Fax: 010-4471884;
Email: stevens.hp@gmail.com

Manuscript received: June 21, 2016
Accepted in final form: September 3, 2016

DOI:10.1111/wrr.12482

Joris A. van Dongen and Hieronymus P. Stevens contributed equally to this work.

ABSTRACT

Autologous adipose tissue transplantation is clinically used to reduce dermal scarring and to restore volume loss. The therapeutic benefit on tissue damage more likely depends on the stromal vascular fraction of adipose tissue than on the adipocyte fraction. This stromal vascular fraction can be obtained by dissociation of adipose tissue, either enzymatically or mechanical. Enzymatic dissociation procedures are time-consuming and expensive. Therefore, we developed a new inexpensive mechanical dissociation procedure to obtain the stromal vascular fraction from adipose tissue in a time sparing way, which is directly available for therapeutic injection. This mechanical dissociation procedure is denoted as the fractionation of adipose tissue (FAT) procedure. The FAT procedure was performed in eleven patients. The composition of the FAT-stromal vascular fraction was characterized by immunohistochemistry. Adipose derived stromal cells isolated from the FAT-stromal vascular fraction were compared with adipose derived stromal cells isolated from nondissociated adipose tissue (control) for their CD-surface marker expression, differentiation and colony forming unit capacity. Case reports demonstrated the therapeutic effect of the FAT-stromal vascular fraction. The FAT-stromal vascular fraction is an enrichment of extracellular matrix containing a microvasculature and culturable adipose derived stromal cells. Adipose derived stromal cells isolated from FAT-stromal vascular fraction did not differ from adipose derived stromal cells isolated from the control group in CD-surface marker expression, differentiation and colony forming unit capacity. The FAT procedure is a rapid effective mechanical dissociation procedure to generate FAT-stromal vascular fraction ready for injection with all its therapeutic components of adipose tissue: it contains culturable adipose derived stromal cells embedded in their natural supportive extracellular matrix together with the microvasculature.

Nowadays, autologous adipose tissue transplantation is frequently used to reduce dermal scarring^{1,2} and to restore volume loss³ as is the case with soft tissue defects, facial fat atrophy^{4,5} and ageing of the face.⁶ The therapeutic benefit of autologous adipose tissue transplantation in these aforementioned situations is partly ascribed to the presence of precursors of adipose derived stromal cells (ASC) in this autologous adipose tissue albeit that this awaits formal proof. ASC are progenitor cells that reside in the stromal vascular fraction (SVF) of adipose tissue attached around the vessels as pericytes and periadventitial cells.^{7,8} In vitro, these precursors readily adhere to tissue culture plastic after their enzymatic dissociation from other cells in the SVF. During culture, the typical ASC phenotype emerges, e.g., the secretion of a plethora of growth factors, cytokines, matrix proteases, and extracellular matrix (ECM) molecules.⁹ Furthermore, these cells are able to differentiate into ectodermal,¹⁰ endodermal,¹¹ or mesenchymal cell-

lineages.¹² Therefore, ASC seem to be suitable for cell-based therapy to repair damaged tissue in organs and aged skin.¹³ For example, in cardiology ASC are already used for the clinical experimental treatment of ischemic cardiomyopathy¹⁴ to repair heart muscle cells, in orthopedics ASC are used to treat intervertebrate disc degeneration¹⁵ and in cosmetic facial surgery ASC are reported to be beneficial for skin rejuvenation.¹⁶

The SVF of adipose tissue comprises all nonadipocyte cells, e.g., fibroblasts, leukocytes, endothelial cells, and the connecting ECM.¹⁷ As a whole, the SVF potentially harbors more therapeutic capacity than the ASC alone: the ECM can augment tissue remodeling, because it acts as a temporary scaffold that also contains matrix remodeling enzymes and because it serves as a slow-release reservoir of growth factors. Moreover, the fragmented microvasculature may augment reperfusion after injection of SVF.^{18–21} Therefore, it would be ideal to harvest this SVF fraction as

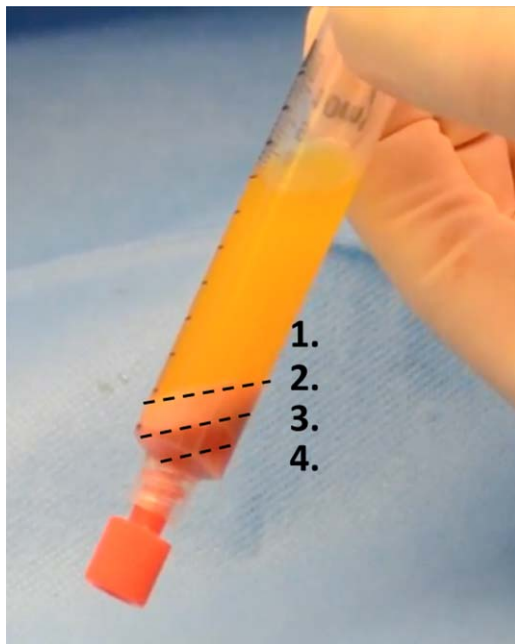


Figure 1. The mechanical dissociation procedure results in four different fractions: (1) oily fraction, (2) SVF and (3) infiltration fluid fraction containing (4) a small pellet fraction. [Color figure can be viewed at wileyonlinelibrary.com]

an intact and injectable “unit” to be used in a more specific way such as in cell-based therapy. This SVF can be isolated from adipose tissue either by means of enzymatic dissociation or by means of mechanical dissociation. Most enzymatic techniques used thus far for isolating the SVF from adipose tissue use collagenase.²² Main disadvantage of all these enzymatic techniques is that they are rather time-consuming and expensive, but also that enzymatic treatment disrupts all communicative connections that exist between the cells as well as between the cells and ECM. Moreover, legislation in several countries does not allow to clinically apply cell-based products that are derived with collagenase.

Mechanical dissociation of adipose tissue to isolate the SVF, however, might be more suitable as compared to enzymatic dissociation, because mechanical dissociation of adipose tissue is a fast time sparing inexpensive method. In this study, we describe a new method to mechanically dissociate adipose tissue intraoperatively to get hold of its therapeutic components for injection: this procedure is named the fractionation of adipose tissue (FAT) procedure.

MATERIALS AND METHODS

Liposuction and FAT procedure

Adipose tissue harvesting was performed with a Sorenson lipo-harvesting cannula (Tulip, Medical Products, San Diego, CA) during normal liposuction procedures in eleven patients (Figure S1, Supporting Information). Adipose tissue was harvested after infiltration with 500 mL-modified

Klein’s solution (per 500 mL of saline, 20 mL of lidocaine, 2% Epinefrine 1 : 200.000 and 2 mL of bicarbonate was added). For the FAT procedure, harvested adipose tissue was centrifuged at 3,000 rpm with a 9.5 cm radius fixed angle rotor for 2.5 minutes (Medilite, Thermo Fisher Scientific, Waltham, MA) at room temperature (RT) after decantation. After one round of centrifugation, the oil and infiltration fluid fractions were discarded, yielding condensed lipoaspirate. One sample of 10 mL of condensed lipoaspirate that was centrifuged only once was used as a control, from hereon referred as “control.” One sample of 10 mL of condensed lipoaspirate was used for mechanical dissociation. For mechanical dissociation, two 10 mL syringes with a total volume of 10 mL of condensed lipoaspirate were connected to the Fractionator, a Luer to Luer transfer with three 1.4 mm holes (Tulip) (Figure S2, Supporting Information). Mechanical dissociation was performed by pushing the lipoaspirate through the Fractionator forward and backwards thirty times (Video S1, Supporting Information). After mechanical dissociation, the adipose tissue was centrifuged again at 3,000 rpm with a 9.5 cm radius fixed angle rotor for 2.5 minutes at RT (Medilite). This resulted in four different fractions: an oily fraction, a SVF (from hereon referred as “FAT-SVF”) and an aqueous fraction containing a small pellet fraction (Figure 1).

Stromal vascular fraction viability

A live dead staining with Carboxyfluorescein Diacetate Succinimidyl Ester (CFDA-SE) and Propidiumiodide (PI) was performed to measure the FAT-SVF viability compared to the control ($n = 3$). For CFDA-SE and PI staining, prewarmed 0.001% of CFDA-SE and 0.001% of PI in serum free Dulbecco’s Modified Eagle’s Medium (DMEM) was used directly on the FAT-SVF and control. After 30 minutes of incubation under culture conditions cells were washed with phosphate buffered saline (PBS) three times and fixed with 2% paraformaldehyde (PFA). DAPI of 0.0002% in PBS was used to stain the nuclei. As a dead cell control, a few samples were fixed with 2% PFA in PBS and then stained with PI. Results were evaluated with a confocal immunofluorescence microscope (Leica TCS SP2 AOBS spectral confocal microscope, Leica Microsystems, Buffalo Grove, IL).

Immunohistochemistry and Masson’s Trichrome

Four of the obtained samples of FAT-SVF and control were formalin-fixed and embedded in paraffin. Four μm of slides were deparaffinized and incubated overnight with 0.1 M Tris/HCL buffer (pH 9.0) for α -Smooth Muscle Actin (α -SMA) and Perilipin A, von Willebrand Factor (vWF) staining was preincubated with 10 mM Tris/1 mM EDTA buffer (pH 9.0). Then, endogenous peroxidase activity was blocked with 30% hydrogen peroxide in PBS for 30 minutes RT. Samples were washed with PBS three times and incubated with primary antibody and 1% bovine serum albumin (BSA) in PBS for 1 hour RT. One percent of human serum (HS) for α -SMA and Perilipin A and 1% swine serum for vWF was added to the primary antibody and 1% BSA. Negative controls were incubated without primary antibodies. Subsequently all samples, including negative controls, were washed with PBS three times and

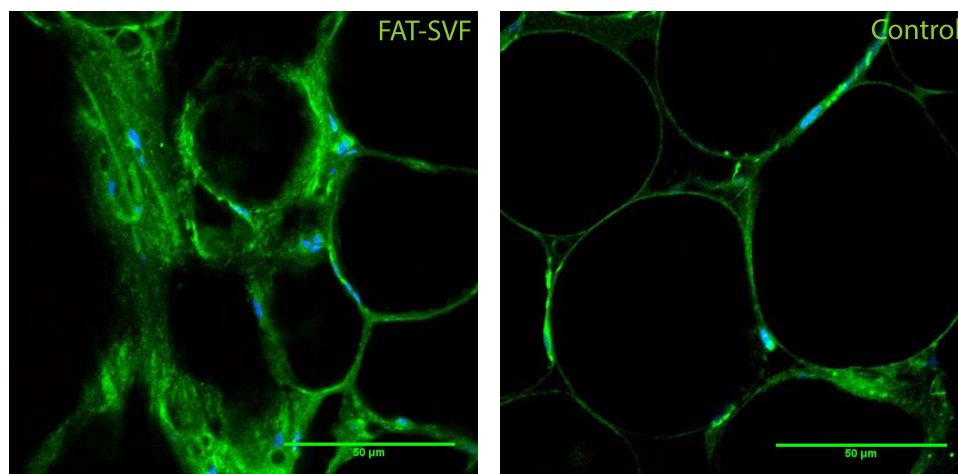


Figure 2. Immunofluorescent images of FAT-SVF and control viability. Living cells turned green, while dead cells turned red after staining with CFDA-SE/PI. Nuclei turned blue after staining with DAPI. [Color figure can be viewed at wileyonlinelibrary.com]

incubated with secondary antibody, 1% BSA, 1% HS in PBS for 30 minutes RT. Only a third antibody in 1% BSA and 1% HS in PBS for 30 minutes was used in α -SMA staining. Staining was completed with 3,3'-diaminobenzidine incubation (Sigma Life Science, St. Louis, MO) and hematoxylin staining of nuclei. Finally, samples were mounted with aqueous mounting agent and visualized under light microscope (Leica Microsystems, DM IL). A Masson's Trichrome staining was performed as well after 4 μ m slides ($n=4$) were deparaffinized. Samples were mounted with toluene solution and visualized under light microscope (Leica Microsystems, DM IL).

Primary antibodies used in this study were directed against alpha smooth muscle actin (α SMA, 1 : 200, Abcam, Cambridge, United Kingdom) to stain smooth muscle cells, vWF (1 : 200, DAKO, Glostrup, Denmark) and Perilipin A (1 : 200, Abcam) to stain adipocytes and. Secondary antibodies used in this study were polyclonal Rabbit anti-mouse for α -SMA (1 : 100, DAKO), polyclonal Swine anti-rabbit for vWF (1 : 100, DAKO) and polyclonal Goat anti-rabbit (1 : 100, DAKO) for Perilipin A. Third antibody used was polyclonal Swine anti-rabbit (1 : 100, DAKO).

Cell isolation and culture

Ten of the obtained samples (FAT-SVF & control) were washed with PBS three times. After washing, 0.1% collagenase A in PBS/1% BSA as dissociation medium was added. The samples were stirred for 1.5 hour in a 37°C water bath. Cells were resuspended in lysisbuffer and placed on ice for 5 minutes to disrupt erythrocytes. The samples were centrifuged at 8°C, 600 \times g for 10 minutes and resuspended in DMEM (BioWhittaker Walkersville, MD): 10% fetal bovine serum (FBS), 1% L-Glutamine, 1% Penicillin/Streptomycin (P/S). Then, seeded in a 6-well plate or 25 cm² tissue culture flask depending on the amount of cells. Cells were counted on staining with trypan blue in a Bürker Turk counting chamber. Cells were cultured at 37°C at 5% CO₂ in a humidified incubator, medium was refreshed twice a week. Morphology of the

cells derived from the FAT-SVF and control were compared after 8 days of culture and visualized with an inverted light microscope with Nomarski phase contrast (Leica Microsystems, DM IL).

Flow cytometry

Cells ($n=6$) collected from cultures after passage 2–4 were analyzed for CD surface marker expression using flow cytometry. Cells were stained with two different sets of anti-human monoclonal antibodies.

Subset A: CD31- phycoerythrine/cyanine7 (Pe/Cy7; IQ Products, Groningen, The Netherlands), CD45-fluorescein isothiocyanate (FITC; IQ Products) and CD90-allophycocyanin (APC; BD Bioscience, San Jose, CA).

Subset B: CD29-APC (eBioscience, Vienna, Austria), CD44-FITC (BD Bioscience) and CD105-Pe/Cy7 (eBioscience). As isotype controls, the following monoclonal antibodies were used: Mouse IgG1 kappa-Pe/Cy7, Mouse IgG1 kappa-APC (both eBioscience) and Mouse IgG1 kappa-FITC (Biolegend, San Diego, CA). Cells were mixed well with each antibody and incubated on ice and in dark for 30 minutes. Isotype cells were used to set the gates on the basis of the staining. A BD FACScalibur system was used to analyze the samples.

Adipogenic, osteogenic, and smooth muscle cell differentiation assay

Cells from passage 2–4 ($n=6$) were collected and cultured in a 24-well plate and incubated in DMEM (containing 10% FBS, 1% L-Glutamine and 1% P/S). After reaching confluence, adipogenic, osteogenic and smooth muscle cell differentiation medium was added to show lipid accumulation, mineralization of bone-like noduli and expression of filamentous actin (F-actin) respectively. Adipogenic differentiation medium consisted of DMEM, 0.1 μ M dexamethasone, 1 nM insulin, 0.5 mM isobutylmethylxanthine. Osteogenic medium consisted of DMEM, 0.1 μ M dexamethasone, 10 mM β -glycerophosphate and 0.05 mM ascorbic acid. Smooth muscle cell differentiation medium consisted of DMEM and 0.1% TGF-beta1. Cells

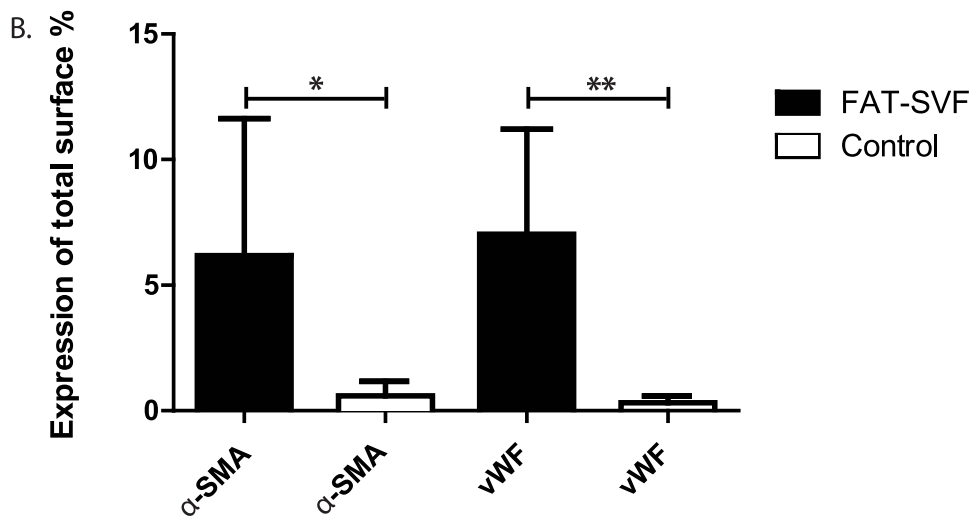
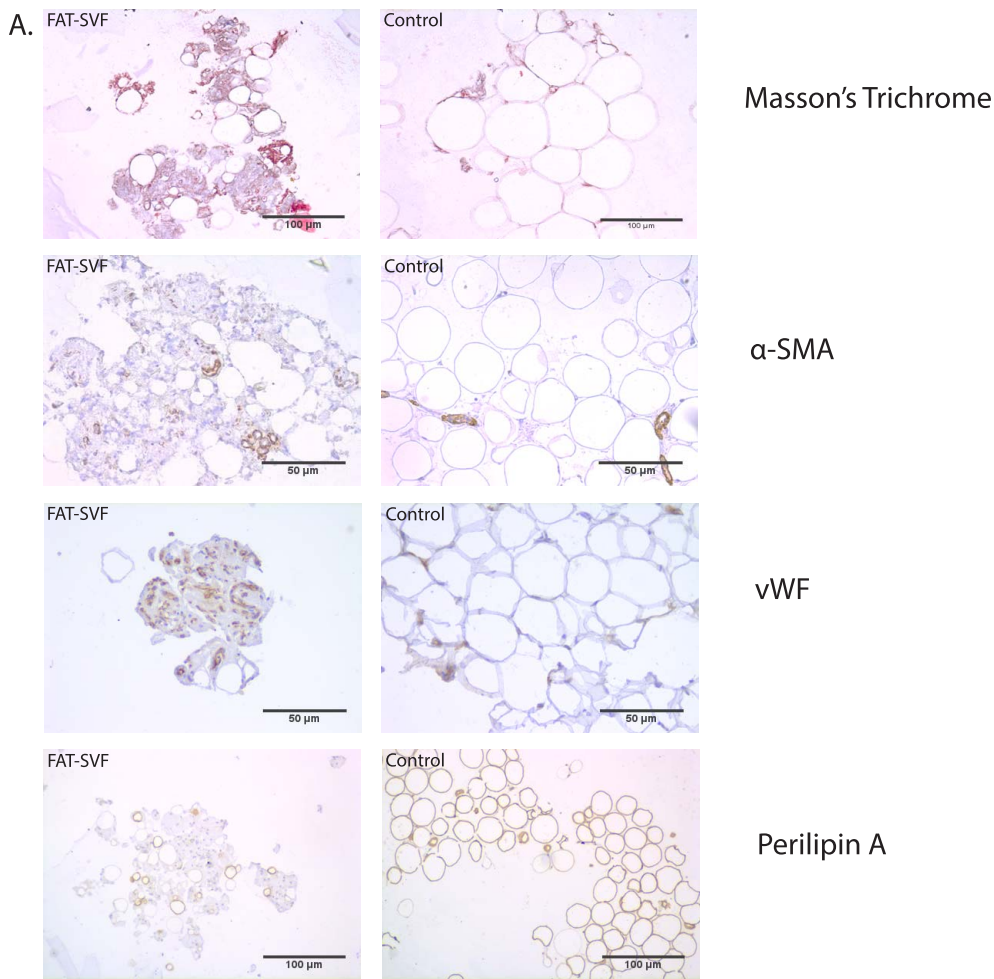


Figure 3. (A) Light microscope images of Masson's Trichrome, α-SMA, vWF, and Perilipin A staining of the FAT-SVF and control samples. (B) Statistic data of expression of α-SMA and vWF in the FAT-SVF as well as in the control. Results are presented as mean ± standard deviation. *Significant more small vessels were visible in the FAT-SVF as compared to the control ($p < 0.05$). **Significant more endothelial cells visible in the FAT-SVF compared to the control ($p < 0.01$). [Color figure can be viewed at wileyonlinelibrary.com]

were cultured in differentiation medium for 14 days. Medium was refreshed twice a week. After 14 days, cells were fixed with 2% PFA and stained with Oil Red O (Sigma-Aldrich, St. Louis, MO) for adipogenic differentiation,

Alizarin Red (Sigma Aldrich) for osteogenic differentiation and Phalloidin-FITC (1 : 250, Invitrogen, Thermo Fisher Scientific) in DAPI for 30 minutes for smooth muscle cell differentiation. Oil Red O staining and Alizarin Red staining

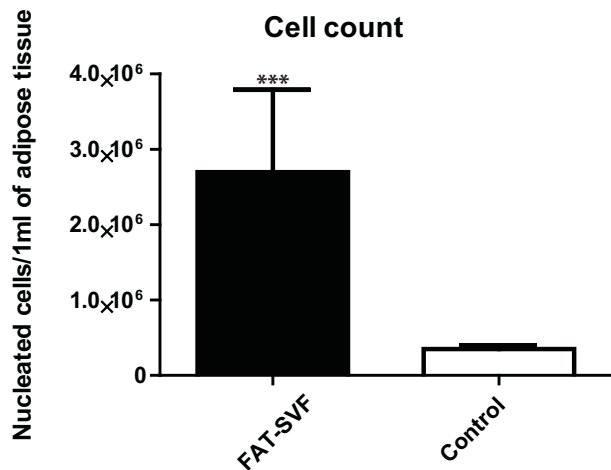


Figure 4. Statistic data of number of nucleated cells per 1 mL of FAT-SVF and control samples. Results are presented as mean \pm standard deviation. *** FAT-SVF contains significant more nucleated cells in 1 mL as compared to 1 mL of control ($p < 0.001$).

were evaluated with a light microscope (Leica Microsystems, DM IL). Phalloidin-FITC staining was evaluated with an immunofluorescence microscope (Leica Microsystems, DM IL).

Colony formation assay

Hundred and thousand cells of FAT-SVF and control ($n = 3$) were plated in a 6-well plate in triplicate and cultured for 14 days. Cell culture plates were washed with PBS three times and fixed with 2% PFA in PBS for 15 minutes. Cells were again washed with PBS three times and stained with 0.05% Crystal Violet (Sigma-Aldrich). After staining, cells were washed with tap water two times and dried inverted. The cloning efficiency or capacity to form colonies from single seeded cells was assessed by determining the area of colonies as well as their intensity of staining with Crystal Violet, both of which are surrogate determinants for the number of cells. Colony area and intensity were analyzed using a plugin for imageJ.²³ Images were taken using Tissue FAXS microscope (TissueGnostics, Vienna, Austria).

Statistical analysis

Immunohistochemistry images and colony formation assay images were analyzed using ImageJ, version 1.4.3.67 (NIH). Descriptive statistics were used to evaluate the cell numbers, α -SMA and vWF expression, CD surface expression scores and colony area and intensity. Data were expressed as mean \pm standard deviation. A *t*-test was performed using Graphpad Prism, version 5.01 (Graph Pad Software Inc., Los Angeles, CA).

RESULTS

Only living cells in the SVF

In the FAT-SVF as well as in the control, only living cells (green) were detected (Figure 2) in contrast to the dead cell (red) controls that contained only dead cells (Figure S3, Supporting Information).

Immunohistochemistry and Masson's Trichrome

The fraction of small vessels visible in FAT-SVF (determined as mean α -SMA positivity of 6.2%, [\pm 5.5] and mean vWF positivity of 7.0%, [\pm 4.2]) was higher than in the controls (mean α -SMA positivity of 0.6%, [\pm 0.6] and mean vWF positivity of 0.3%, [\pm 0.3]), respectively $p < 0.05$ and $p < 0.01$ (Figure 3). Interestingly, in both groups, vessels were present that did not express vWF. Likely, the procedure to generate the FAT-SVF had activated part of the vessels and caused these to release their vWF. vWF and other "damage-response" proteins, are stored in the Weibel Palade bodies within endothelial cells, the contents of which are secreted after stress-induced activation such mechanical shear. Therefore, only quantification of vWF was performed on samples that expressed vWF staining, implying the presence of nonactivated EC. Perilipins are lipid-coating proteins that protect against lipase action. Therefore, the presence of Perilipin marks intact adipocytes. After mechanical dissociation, adipocyte "ghosts" were present in the FAT-SVF occasionally (Figure 3). Mainly large adipocytes were visible in the control, whereas only smaller ones in the FAT-SVF. Masson's Trichrome staining showed more collagen deposition (blue) between the cells (red) in the FAT-SVF as compared to the control (Figure 3), implying enrichment of ECM in the FAT-SVF by disrupting adipocytes compared to controls.

Mechanical dissociation cell yield

Complete mechanical dissociation of adipose tissue was performed intraoperatively within 8 to 10 minutes of extra operating time and resulted in a FAT-SVF with a mean volume of 0.96 mL [range 0.75 to 1.75]. Enzymatic isolation of the FAT-SVF resulted in a mean number of cells of 2.7×10^6 [\pm 1.1×10^6] per 1 mL (Figure 4). Enzymatic isolation of 10 mL of the control resulted in a mean number of cells of 3.5×10^5 [\pm 5.1×10^6] per 1 mL ($p < 0.001$), a 7.7 times lower number of cells in 1 mL adipose tissue as compared to 1 mL of FAT-SVF (Figure 4). Three patients were excluded from the study. One patient had an uncountable low number of cells in the FAT-SVF sample. In one FAT-SVF and one control sample of two different patients, we were unable to culture enough cells to reach confluency. Cultured cells had a spindle-shaped fibroblast-like morphology in both samples (Figure S4, Supporting Information). There was no visible difference between both groups.

Cells cultured from mechanically dissociated adipose tissue harbor ASC characteristics

For subset A, a mean of 99.8% [\pm 0.2] of the FAT-SVF showed expression of CD90 and no expressions of CD31

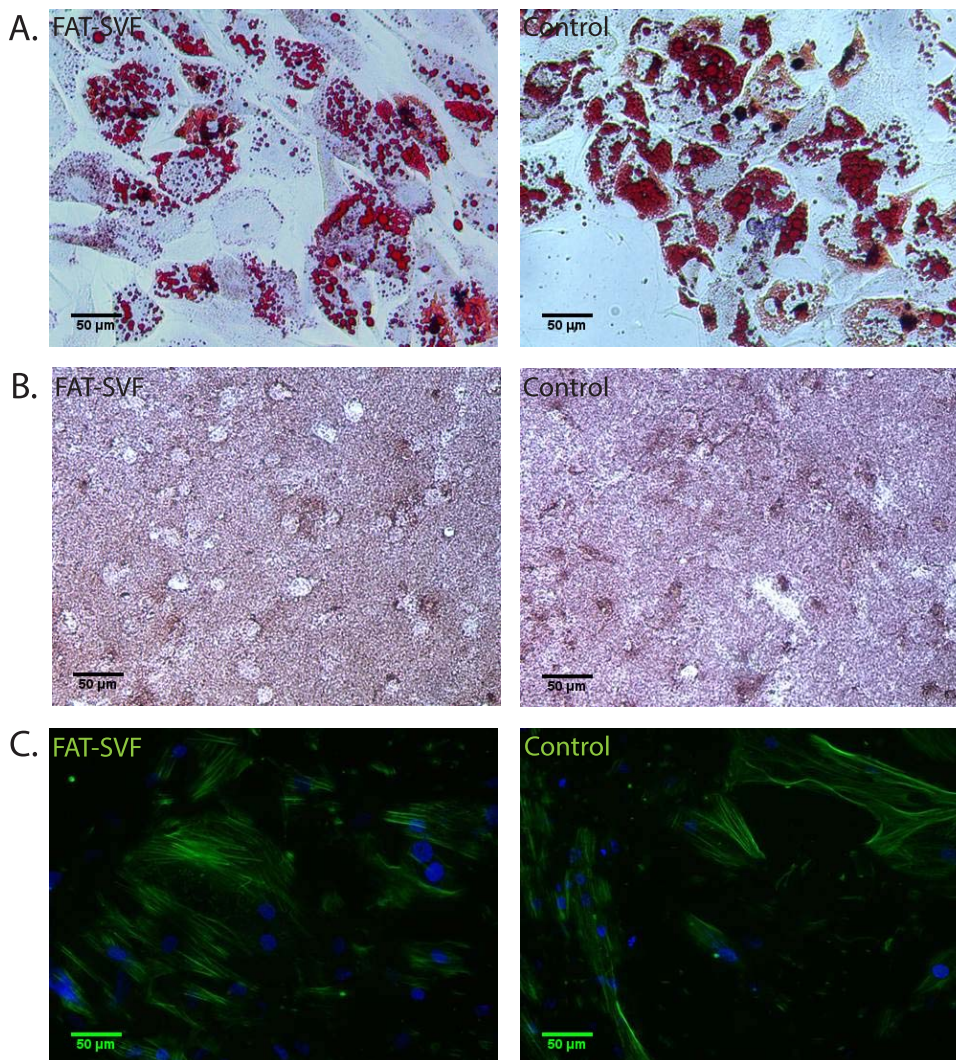


Figure 5. Light microscope and immunofluorescent images of ASC derived from FAT-SVF and control. (A) After Oil Red O staining, lipid droplet accumulation turned red. (B) After Alizarin Red staining, mineralized bone-like nodules turned red. (C) After phalloidin-FITC staining, F-actin turned green. No visual differences between FAT-SVF and control. [Color figure can be viewed at wileyonlinelibrary.com]

and CD45 were shown. For the control, a mean of 99.8% [± 0.1] showed expression of CD90 with also no expressions of CD31 and CD45. There was no significant difference between the two groups ($p > 0.05$).

For subset B, a mean of 99.8% [± 0.2], 99.0% [± 0.7] and 95.9% [± 4.5] of the FAT-SVF showed expression of CD29, CD44, and CD105. For the control, a mean of 98.2% [± 3.5], 98.5% [± 1.2] and 96.6% [± 2.6] showed expression of CD29, CD44, and CD105, respectively. No significant differences occurred between the two groups ($p > 0.05$). Representative data of CD-surface marker expression is shown in Figure S5, Supporting Information.

Cells cultured from FAT-SVF retain adipogenic, osteogenic and smooth muscle cell differentiation capacity

All samples of the FAT-SVF and the control showed significant more lipid droplet formation, mineralized bone-like noduli formation and f-actin expression compared to

their negative controls (Figure S6, Supporting Information). No significant differences were present between the FAT-SVF and the control (Figure 5). As ASC are known to express F-actin in all cases, all negative controls were slightly positive as anticipated. One sample of the control group detached, most likely due to contraction of F-actin.

Cells from FAT-SVF retain colony formation capacity

Total colony areas and colony intensities did not differ between ASC derived from the FAT-SVF and controls. This was irrespective of the initial seeding density ($p > 0.05$) (Figure 6).

DISCUSSION

In this study, we have demonstrated that the FAT procedure is both efficient and reliable intra-operative method to isolate the FAT-SVF from adipose tissue within 8 to 10 minutes in a simple and reproducible way, suitable for

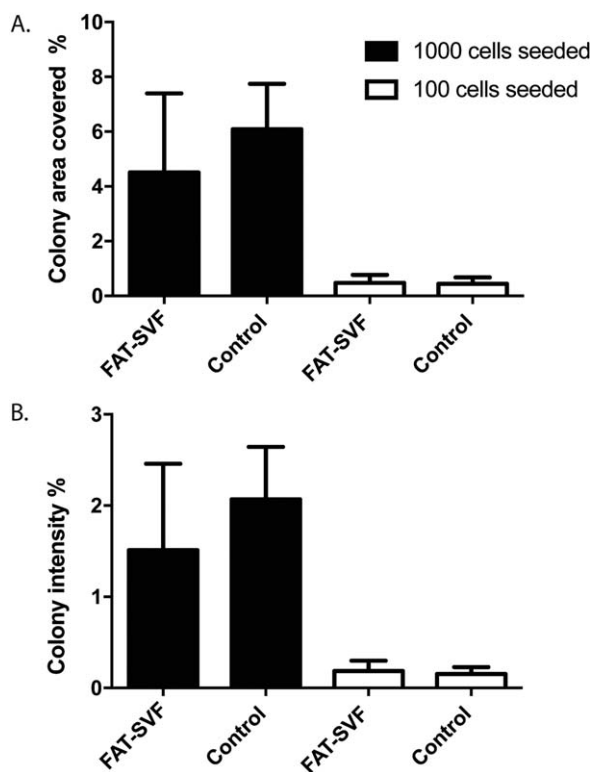


Figure 6. Statistic data of (A) total colony area covered and (B) colony intensity of ASC derived from FAT-SVF and control. No significant differences in colony area covered and intensity between ASC derived from FAT-SVF and control when hundred or thousand cells were seeded ($p > 0.05$).

injection: the FAT procedure dissociates lipoaspirate by disrupting adipocytes mechanically and consequently results in a SVF containing culturable ASC as well as small vessels embedded in an ECM. This FAT-SVF is indicated to increase scar remodeling and might even accelerate wound healing *in vivo*.

ASC derived from the FAT-SVF as well as ASC from the control showed similar expression with regard to the CD-surface markers, had similar like spindle shaped fibroblast-like morphology, the same multipotent differentiation potential and colony formation capacity.

Phenotypically, ASC have two main characteristics. First, ASC possess markers such as mesenchymal markers (CD29+, CD44+, CD90+, and CD105+) and endothelial and hematopoietic markers (CD31- and CD45-, respectively).²⁴ ASC freshly isolated from adipose tissue are CD105-, but become CD105+ after culturing.¹⁷ Therefore, the variation of CD105+ cells can be larger than for other CD surface markers. Furthermore, endothelial cells also express CD105, which is TGF-beta receptor type III, which might influence the FACS results.¹⁷ Second, ASC are able to attach to culture plastic flasks and present as having a spindle shaped fibroblast-like morphology. Functionally, ASC are characterized by their ability to differentiate into adipocytes, osteoblasts and smooth muscle cells.^{12,24} As there are no significant or visual differences in function and phenotype between ASC derived from the

SVF and the control, the FAT procedure apparently does not affect the potential of ASC. Furthermore, the FAT procedure results in a FAT-SVF that contains only living cells and significantly more nucleated cells in 1 mL of adipose tissue as compared to nondissociated lipoaspirate.

The FAT procedure is a reproducible method to generate consistent volumes of injectable FAT-SVF. The composition of the FAT-SVF is histologically heterogeneous: some parts consist of small blood vessels mainly, while other parts consist of ECM only. We surmise that the mechanical disruption of the adipose tissue causes a redistribution of softer (ECM) and harder (microvasculature) component of the FAT-SVF. The heterogeneity, however, could also be a consequence of inter-patient variation. For this study anonymized samples were obtained. Therefore, future clinical trials might reveal variation among patients. vWF staining was only present in the nonactivated endothelial cells in the FAT-SVF. Activated endothelial cells secrete their vWF and respond, therefore, negative to the vWF staining. The ratio between activated and non-activated endothelial cells, however, remains unclear. Quantification of the number of adipocytes as compared to the surface area of FAT-SVF proved methodologically to be impossible. When all adipocytes are mechanically disrupted, the FAT-SVF disintegrates into small unquantifiable parts. When a few adipocytes are still intact, bigger parts of FAT-SVF are visible. In this way only quantification of the bigger parts of FAT-SVF, containing more adipocytes, is possible. So therefore, the number of adipocytes counted is higher as compared to the real number of adipocytes. Interestingly, our method to disrupt adipose tissue yielded an injectable FAT-SVF that contains all the prerequisites for tissue regeneration: ASC, microvasculature and supporting ECM.

Compared to conventional or automated dissociation methods of adipose tissue, the FAT procedure is a faster and more cost-effective method to produce a FAT-SVF.²⁵ The dissociation device is small and of simple design, i.e., even in disposable format can be produced cost effective, in particular in large quantities. The short time necessary for the mechanical dissociation procedure enables the surgeon to use the FAT-SVF during surgery with a minimal delay of operation time. It also likely contributes to the high vitality of cells that are retained in the FAT-SVF. As opposed to enzymatic digestion, where ASC need to survive in an ischemic environment due to the lengthy isolation procedure. Also the use of collagenase or non-autologous material potentially renders enzymatic digestion more sensitive for (bacterial) contamination. Furthermore, enzymatic isolation results in a SVF comprised of a suspension of individual, nonconnected cells with a total lack of tissue structure. In general, retention rates of single cell injections (i.e., ASC) are rather low.²⁶ With mechanical dissociation, the ECM is retained in the FAT-SVF, which probably functions as a "microvascularized" scaffold for the ASC thus keeping a matrix for tissue integrity. In this way, it can be expected to increase cell survival after injection, thus reducing the otherwise low reported retention rates.

The interaction between cells and growth factors in FAT-SVF is expected to increase the regenerative potential in cell-based therapy as compared to the single use of ASC. For instance, the combined application of pericytes

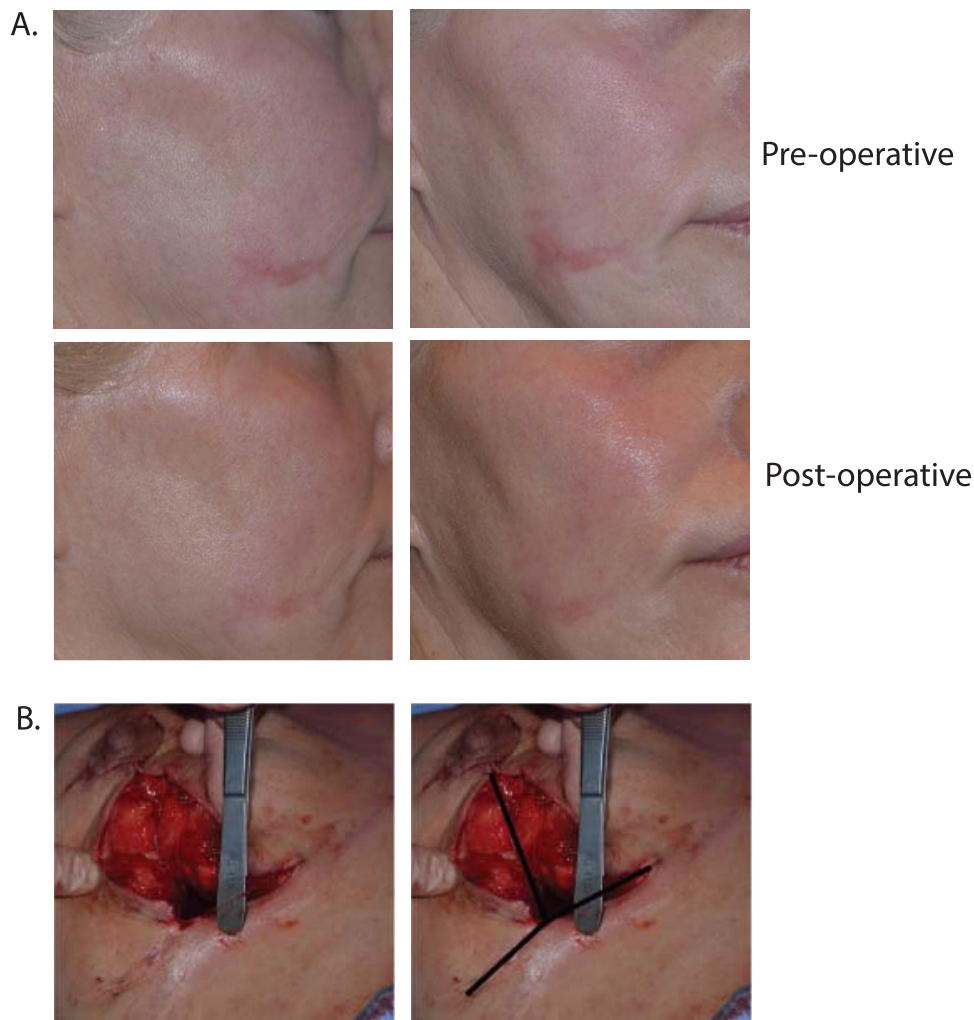


Figure 7. (A) A 62-year-old female patient with a nine-month-old scar as a result of a too deep TCA peeling. After injection with FAT-SVF, the dark red colorization of the scar became brighter and resembled to normal skin. (B) A 33-year-old female patient with partial dehiscence of the wounds, 2 weeks postoperative after a mamma reduction. The lateral 5 cm of the horizontal scar was injected with FAT-SVF after the mamma reduction and remained closed. Barbed V-lock suture is still intact and visible in first image. Black lines mark the place of the suture in the second image. [Color figure can be viewed at wileyonlinelibrary.com]

and endothelial cells has been shown to augment angiogenesis compared to their single use.²⁷ Additionally, ASC enhance angiogenesis through secreted growth factors such as vascular endothelial growth factor (VEGF), fibroblast growth factor(s) (FGF), and hepatocyte growth factor (HGF),^{28,29} in particular under hypoxia.²⁰ ASC conditioned medium, which is rich in VEGF, FGFs, and HGF, both increases the proliferation rate of endothelial cells, while suppressing apoptosis, in particular under hypoxia.²⁹ Endothelial cell proliferation and survival are important mechanisms in angiogenesis.³⁰ Furthermore, the ECM in FAT-SVF influences the migration and morphogenesis of angiogenesis.³¹ ECM contains several proteins such as collagen and fibronectin, which are important during the wound healing process.³² Hence, we surmise that FAT-SVF might also be a suitable cell-based therapy for stimulating wound healing or regeneration of damaged tissue, as we already have experienced in two illustrative cases (rest of series will be published when the prospective clinical trials have been finished). Firstly, a 62-year-old female patient suffered for nine months from prolonged redness and scar formation on her right cheek after a too deep peeling with

trichloroacetic acid (TCA) that did not want to subside. Within 3 weeks after injection with 1 mL of FAT-SVF, the deep red colored scar became brighter and turned into nearly normal skin (Figure 7). In the second case, a 33-year-old female patient received an injection of FAT-SVF in the lateral 5 cm of the horizontal incision after a mamma reduction. Two weeks postoperative, full dehiscence of the wounds occurred, after cheese wiring of the barbed suture, except for the area treated by FAT-SVF (Figure 7).³³ Probably, FAT-SVF injection accelerated wound healing, making the premature scar better resistant to mechanical forces in an earlier phase during wound repair compared to the nontreated wound edges.

Autologous adipose tissue transplantation to replace lost volume or to improve wound healing and revise dermal scars, i.e., fibrotic lesions is routinely performed nowadays. Ideally, anti-scar treatment would resolve the existing scar which would involve the degradation of excessively deposited ECM, the removal of unwanted cells such as myofibroblasts and finally the restoration of the original tissue architecture of the dermis including its subcutaneous adipose tissue. We argue that initially the filler

effect of fat grafts is less relevant than its anti-scarring properties. Thus, enrichment of anti-scarring cells or matrix, which are both present in the FAT-SVF, might favor the process. At later stages, the precursor cells of adipocytes that reside within FAT-SVF, will regenerate the subcutaneous adipose tissue. Treatment of fibrosis in organs such as heart, kidney or liver, or in osteoarthritic joints such a knee or temporomandibular, with bulky lipografts is undesirable, due to tissue damage caused by injection of large volumes. Therefore, the reduction of the volume of lipoaspirate, as can be achieved with our FAT procedure, to generate an injectable ECM-based cellularized therapeutic gel, that act as an instructive scaffold for repair, seems to be a promising alternative.

CONCLUSION

The FAT procedure is an effective method to mechanically dissociate lipoaspirate and to create a FAT-SVF with all the therapeutic components of adipose tissue in about 10% of its original volume during a surgical procedure without hardly any time-loss: it contains a 7.7 times higher number of nucleated cells as compared to nondissociated lipoaspirate and ASC embedded in an ECM that also contains a microvasculature structure.

Further prospective studies are necessary to assess the therapeutic value of the FAT-SVF as such, for e.g., in organ repair, scar revision, osteoarthritis, or wound healing. Currently, we are conducting two double blind randomized clinical trials to assess this effect of FAT-SVF on scar formation and skin quality.

ACKNOWLEDGMENTS

Disclosure: None of the authors has a financial interest in any of the products, devices, or drugs mentioned in this manuscript.

Source of Funding: No funding was received to assist in the creation of this manuscript.

Conflicts of Interest: The authors have no conflict of interest to disclose in relation to the content of this work.

REFERENCES

1. Brongo S, Nicoletti GF, La Padula S, Mele CM, D'Andrea F. Use of lipofilling for the treatment of severe burn outcomes. *Plast Reconstr Surg* 2012; 130 (2): 374e–6e.
2. Pallua N, Baroncini A, Alharbi Z, Stromps JP. Improvement of facial scar appearance and microcirculation by autologous lipofilling. *J Plast Reconstr Aesthet Surg* 2014;67 (8): 1033–7.
3. Largo RD, Tchang LA, Mele V, Scherberich A, Harder Y, Wettstein R, et al. Efficacy, safety and complications of autologous fat grafting to healthy breast tissue: a systematic review. *J Plast Reconstr Aesthet Surg* 2014; 67 (4): 437–48.
4. Agostini T, Spinelli G, Marino G, Perello R. Esthetic restoration in progressive hemifacial atrophy (Romberg disease): structural fat grafting versus local/free flaps. *J Craniofac Surg* 2014; 25 (3): 783–7.
5. Tanna N, Broer PN, Roostaeian J, Bradley JP, Levine JP, Saadeh PB. Soft tissue correction of craniofacial microsomia and progressive hemifacial atrophy. *J Craniofac Surg* 2012; 23 (7 Suppl 1): 2024–7.
6. Willemsen JC, Mulder KM, Stevens HP. Lipofilling with minimal access cranial suspension lifting for enhanced rejuvenation. *Aesthet Surg J* 2011; 31 (7): 759–69.
7. Corselli M, Chen CW, Sun B, Yap S, Rubin JP, Peault B. The tunica adventitia of human arteries and veins as a source of mesenchymal stem cells. *Stem Cells Dev* 2012; 21 (8): 1299–308.
8. Lin G, Garcia M, Ning H, Banie L, Guo YL, Lue TF, et al. Defining stem and progenitor cells within adipose tissue. *Stem Cells Dev* 2008; 17 (6): 1053–63.
9. Pawitan JA. Prospect of stem cell conditioned medium in regenerative medicine. *BioMed Res Int* 2014; 2014: 965849.
10. Ferroni L, Gardin C, Tocco I, Epis R, Casadei A, Vindigni V, et al. Potential for neural differentiation of mesenchymal stem cells. *Adv Biochem Eng Biotechnol* 2013; 129: 89–115.
11. Baer PC. Adipose-derived stem cells and their potential to differentiate into the epithelial lineage. *Stem Cells Dev* 2011; 20 (10): 1805–16.
12. Zuk PA, Zhu M, Ashjian P, De Ugarte DA, Huang JL, Mizuno H, et al. Human adipose tissue is a source of multipotent stem cells. *Mol Biol Cell* 2002;13 (12):4279–95.
13. Nery AA, Nascimento IC, Glaser T, Bassaneze V, Krieger JE, Ulrich H. Human mesenchymal stem cells: from immunophenotyping by flow cytometry to clinical applications. *Cytometry Part A* 2013; 83 (1): 48–61.
14. Perin EC, Sanz-Ruiz R, Sanchez PL, Lasso J, Perez-Cano R, Alonso-Farto JC, et al. Adipose-derived regenerative cells in patients with ischemic cardiomyopathy: The PRECISE Trial. *Am Heart J* 2014; 168 (1): 88–95.e2.
15. Yim RL, Lee JT, Bow CH, Meij B, Leung V, Cheung KM, et al. A systematic review of the safety and efficacy of mesenchymal stem cells for disc degeneration: insights and future directions for regenerative therapeutics. *Stem Cells Dev* 2014; 23 (21): 2553–67.
16. Charles-de-Sa L, Gontijo-de-Amorim NF, Maeda Takiya C, Borojevic R, Benati D, Bernardi P, et al. Antiaging treatment of the facial skin by fat graft and adipose-derived stem cells. *Plast Reconstr Surg* 2015; 135 (4): 999–1009.
17. Yoshimura K, Shigeura T, Matsumoto D, Sato T, Takaki Y, Aiba-Kojima E, et al. Characterization of freshly isolated and cultured cells derived from the fatty and fluid portions of liposuction aspirates. *J Cell Physiol* 2006; 208 (1): 64–76.
18. Bosman FT, Stamenkovic I. Functional structure and composition of the extracellular matrix. *J Pathol* 2003; 200 (4): 423–8.
19. Semon JA, Zhang X, Pandey AC, Alandete SM, Maness C, Zhang S, et al. Administration of murine stromal vascular fraction ameliorates chronic experimental autoimmune encephalomyelitis. *Stem Cells Transl Med* 2013; 2 (10): 789–796.
20. Atalay S, Coruh A, Deniz K. Stromal vascular fraction improves deep partial thickness burn wound healing. *Burns* 2014; 40 (7): 1375–83.
21. Premaratne GU, Ma LP, Fujita M, Lin X, Bollano E, Fu M. Stromal vascular fraction transplantation as an alternative therapy for ischemic heart failure: anti-inflammatory role. *J Cardiothorac Surg* 2011; 6: 43.
22. Zuk PA, Zhu M, Mizuno H, Huang J, Futrell JW, Katz AJ, et al. Multilineage cells from human adipose tissue: implications for cell-based therapies. *Tissue Eng* 2001; 7 (2): 211–28.
23. Guzman C, Bagga M, Kaur A, Westermarck J, Abankwa D. ColonyArea: an ImageJ plugin to automatically quantify colony formation in clonogenic assays. *PLoS One* 2014; 9 (3): e92444.

24. Bourin P, Bunnell BA, Casteilla L, Dominici M, Katz AJ, March KL, et al. Stromal cells from the adipose tissue-derived stromal vascular fraction and culture expanded adipose tissue-derived stromal/stem cells: a joint statement of the International Federation for Adipose Therapeutics and Science (IFATS) and the International Society for Cellular Therapy (ISCT). *Cytotherapy* 2013; 15 (6): 641–8.
25. Aronowitz JA, Ellenhorn JD. Adipose stromal vascular fraction isolation: a head-to-head comparison of four commercial cell separation systems. *Plast Reconstr Surg* 2013; 132 (6): 932e–9e.
26. Parvizi M, Harmsen MC. Therapeutic prospect of adipose-derived stromal cells for the treatment of abdominal aortic aneurysm. *Stem Cells Dev* 2015; 24 (13): 1493–505.
27. Traktuev DO, Prater DN, Merfeld-Clauss S, Sanjeevaiah AR, Saadatzadeh MR, Murphy M, et al. Robust functional vascular network formation in vivo by cooperation of adipose progenitor and endothelial cells. *Circ Res* 2009; 104 (12): 1410–20.
28. Cai L, Johnstone BH, Cook TG, Liang Z, Traktuev D, Cornetta K, et al. Suppression of hepatocyte growth factor production impairs the ability of adipose-derived stem cells to promote ischemic tissue revascularization. *Stem Cells (Dayton, Ohio)* 2007; 25 (12): 3234–43.
29. Rehman J, Traktuev D, Li J, Merfeld-Clauss S, Temm-Grove CJ, Bovenkerk JE, et al. Secretion of angiogenic and antiapoptotic factors by human adipose stromal cells. *Circulation* 2004; 109 (10): 1292–8.
30. Chavakis E, Dimmeler S. Regulation of endothelial cell survival and apoptosis during angiogenesis. *Arterioscler Thromb Vasc Biol* 2002; 22 (6): 887–93.
31. Bauer AL, Jackson TL, Jiang Y. Topography of extracellular matrix mediates vascular morphogenesis and migration speeds in angiogenesis. *PLoS Comput Biol* 2009; 5 (7): e1000445.
32. Midwood KS, Williams LV, Schwarzbauer JE. Tissue repair and the dynamics of the extracellular matrix. *Int J Biochem Cell Biol* 2004; 36 (6): 1031–7.
33. Cravy TV. A modified suture placement technique to avoid suture drag or “cheese wire” effect. *Ophthalmic Surg* 1980; 11 (5): 338–42.

Supporting Information

Additional Supporting Information may be found in the online version of this article.